INSTITUTE OF PLASMA PHYSICS

NAGOYA UNIVERSITY

Strong Ion Accelerating by Collisionless Magnetosonic shock Wave Propagating Perpendicular to a Magnetic Field

Yukiharu Ohsawa

(Received – Dec. 5, 1984)

IPPJ- 709 Dec. 1984

RESEARCH REPORT

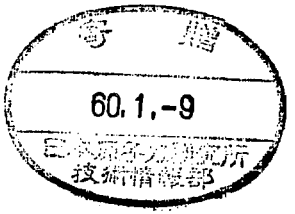

NAGOYA, JAPAN

Strong Ion Accelerating by Collisionless Magnetosonic shock Wave Propagating Perpendicular to a Magnetic Field

Yukiharu Ohsawa

(Received - Dec. 5, 1984)

IPPJ- 709 Dec. 1984

Further communication about this report is to be sent to the Research Information Center, Institute of Plasma Physics, Nagoya University, Nagoya 464, Japan.

Abstract

A 2-1/2 dimensional fully relativistic, fully electromagnetic particle code is used to study a time evolution of nonlinear magnetosonic pulse propagating in the direction perpendicular to a magnetic field. The pulse is excited by an instantaneous piston acceleration, and evolves totally self-consistently. Large amplitude pulse traps some ions and accelerates them parallel to the wave front. They are detrapped when their velocities become of the order of the sum of the $E\times B$ drift velocity and the wave phase velocity, where E is the electric field in the direction of wave propagation. The pulse develops into a quasi-shock wave in a collisionless plasma by a dissipation due to the resonant ion acceleration. Simple nonlinear wave theory for a cold plasma well describes the shock properties observed in the simulation except for the effects of resonant ions. In particular, magnitude of an electric potential across the shock region is derived analytically and is found to be in good agreement with our simulations. The potential jump is proportional to B^2, and hence the $E\times B$ drift velocity of the trapped ions is proportional to B.

I. Introduction

It was shown theoretically by Sugihara and Midzuno[1,2] that a strong monochromatic electrostatic wave propagating perpendicular to an external magnetic field can strongly accelerates the ions parallel to the wave front within a short time period, $t \sim O(\omega^{-1}_{ci})$ where ω_{ci} is the ion cyclotron frequency. The large amplitude wave traps some particles whose velocities are around the wave phase velocity, and accelerates them in the direction of the wave propagation, say in the x-direction. The increased velocity v_x is continuously converted to the velocity v_y by the Lorentz force; here we have assumed that the wave propagates in the x-direction with the external magnetic field in the z-direction. Hence, the velocity v_x of the resonant particles can stay long around the wave phase velocity v_p; the resonant particles can interact with the electric field E_x of the wave much longer than the ion cyclotron period or the bounce time in the wave trough. They are detrapped when the kinetic energy is so large that the Lorentz force overcomes the electric force of the wave. In this paper we call this acceleration mechanism the $v_p \times B$ acceleration.

Recently Lembege *et al*[3,4] investigated, by means of a one dimensional electromagnetic particle simulation, the $v_p \times B$ acceleration by a large-amplitude monochromatic magnetosonic wave. They observed that some ions are accelerated and trapped in the potential troughs of the wave, and as the theory predicts the particles are accelerated parallel to the wave front.

In the theories of Refs.(1) and (2), they assumed that there is a monochromatic electric field with constant amplitude, $E_x = E_0 \sin(kx - \omega t)$, in a magnetized plasma. Also, in the simulations of Refs.(3) and (4), they imposed a propagating external current with constant amplitude,

$j_y=j_0 sin(kx-\omega t)$, to excite the magnetosonic wave. Hence the waves treated in their theory and simulation were not totally self-consistent. Then, some natural questions arise. What is the electric field strength of the self-consistent nonlinaer magnetosonic wave ? Does the self-consistent wave really give rise to the $v_p \times B$ acceleration ? The profile and the propagation speed of the nonlinear wave may also quite different from those of the monochromatic (linear) wave.

In the present paper we study the magnetosonic shock wave[5-9] propagating in the direction perpendicular to the magnetic field by using a 2-1/2 dimensional electromagnetic particle code[10], with particular attension to the $v_p \times B$ acceleration of the ions at the shock region. A large-amplitude magnetosonic pulse is excited by a sort of piston acceleration perpendicular to the magnetic field at time $t=0$. The pulse thus excited develops into a quasi-shock wave. The plasma density and the magnetic field rise rapidly in the shock region, and they gradually decrease behind the shock region; they have the saw-tooth structure.

It is interesting to note that the magnetosonic shock wave appears in a collisionless plasma. Morawetz[9] pointed out that shock solutions can be found in the absence of collisions if there are a number of ions which bounce off the shock front before passing through the shock. In our case the $v_p \times B$ acceleration of the resonant particles plays a role of dissipation. If there are no dissipation mechanisms, the pulse would develops into a soliton[11,12].

The time evolution of the shock wave after the piston acceleration is totally self-consistent; no external electric fields nor currents are imposed. It is confirmed that the propagation velocity of the shock increases with the strength of pulse. For the strong pulse, a large electric potential is formed across the shock region, which results in the

$v_p \times B$ acceleration of the trapped ions.

In Sec.II, on the basis of the simple nonlinear wave theory for the cold plasma we derive an expression for the electric potential profile in terms of the magnetic field and the plasma variables ahead of the shock. The potential difference can be quite large compared to the ion temperature unless the Alfven Mach number of the nonlinear pulse is too close to unity. The potential difference is proportional to B^2, and hence the $E \times B$ drift velocity of the trapped ions is proportional to B. We describe the simulation model in Sec.III. Simulation results are given in Sec.IV. It is demonstrated that the self-consistent nonlinear pulse develops into the quasi-shock wave in a collisionless plasma and that the nonlinear pulse generates many high-energy ions by the $v_p \times B$ acceleration. Propagation properties of the shock are compared with the nonlinear wave theory. We summarize our results in Sec.V.

II. Estimation of Electric Field Strength

In this section we calculate the magnitude of the elctric field E_z in a nonlinear magnetosonic wave propagating in the direction perpendicular to the magnetic field. The estimated electric field is very large, which implies that the $v_p \times B$ acceleration can occur in the magnetosonic shock wave (or soliton). The nonlinear magnetosonic wave has been investigated theoretically by many authers, and here we follow the simplest method[8].

We consider a steady propagation of the nonlinear magnetosonic wave in a dissipationless cold plasma. We assume that the magnetic field points in the z-direction and the wave is propagating in the positive x-direction. In the wave-frame where the time-derivatives are zero, we

have the relationship for the density n and the velocity v_x from the continuity equations for the ions and electrons,

$$n_j v_{xj} = n_{1j} v_{1j} = n_1 v_1 , \tag{1}$$

where the subscript 1 refers to the plasma variables at x=∞, and the j denotes the ions or the electrons. Quasi neutrality condition leads to the following equations,

$$v_{xi} = v_{xe} = v_x . \tag{2}$$

It follows from Faraday's law that the electric field E_y is independent of x, and is given by

$$E_y = v_1 B_1 / c , \tag{3}$$

where c is the light velocity. The momentum equations and Ampere's law can be written as,

$$v_x dv_x/dx = (q_j/m_j) E_x + (q_j/m_j c) v_{yj} B , \tag{4}$$

$$v_x dv_{yj}/dx = (q_j/m_j) E_y - (q_j/m_j c) v_x B , \tag{5}$$

$$-dB/dx = (4\pi/c)(n_i q_i v_{yi} + n_e q_e v_{ye}) . \tag{6}$$

Combining these equations, we have the electric field E_x in terms of the magnetic field and the quantities ahead of the shock,

$$E_x = -(dB^2/dx)(1 - (B^2 - B_1^2)/8\pi n_1 m_i v_1^2)/8\pi n_1 q_i , \tag{7}$$

and the ion velocity in the y-direction is

$$v_{yi} = (m_e/m_i) c E_x / B . \tag{8}$$

Integration of Eq.(7) yields the potential difference,

$$q_i(\varphi(x)-\varphi_1)=(m_i v_{a1}^2/2)\{(1+1/2M_a^2)[(B/B_1)^2-1]-(1/4M_a^2)[(B/B_1)^4-1]\}, \quad (9)$$

where v_a is the Alfven velocity, $v_a=B/(4\pi n m_i)^{1/2}$, and M_a is the Alfven Mach number, $M_a=v_1/v_{a1}$. For the magnetosonic soliton in a cold dissipationless plasma[8], the ratio of the maximum magnetic field B_m to B_1 is related to the Alfven Mach number as $B_m/B_1=2M_a-1$. Substituting this relationship into Eq.(9) leads to

$$q_i(\varphi_m-\varphi_1)=2m_i v_{a1}^2(M_a-1), \quad (10)$$

or

$$q_i(\varphi_m-\varphi_1)=m_i v_{a1}^2((B_m/B_1)-1), \quad (10')$$

where φ_m is the peak value of the potential.

Equation (9) or (10) indicates that for a low beta plasma where the ion thermal velocity is much smaller than the Alfven velocity, $v_{ti}\ll v_a$, the potential energy formed by the nonlinear magnetosonic wave can be much larger than the average kinetic energy unless the Alfven Mach number is too close to unity.

Since the soliton width is given by[8]

$$\Delta=(c/\omega_{pe})(2(M_a-1))^{-1/2}, \quad (11)$$

we have the rough estimation for the magnitude of the electric field E_x as

$$q_i E_x \sim m_i v_{a1}^2(M_a-1)^{3/2}/(c/\omega_{pe}). \quad (12)$$

According to the theory by Sugihara and Midzuno[1], if there is an

electrostatic wave propagating perpendicular to the external magnetic field with the frequency range of the ion cyclotron frequency ω_{ci}, some ions with the velocity near the wave phase velocity can be trapped and strongly accelerated in the y-direction. The ions will be detrapped when the velocity becomes of the order of the $E\times B$ drift velocity. Equation (10) or (10') implies that the electric potential in the the nonlinear magnetosonic wave can be large enough to trap the ions. If the $v_p\times B$ acceleration occurs to the trapped ions, the ions will be accelerated up to

$$v\sim (v_{a1}^2/c)(M_a-1)^{3/2}\omega_{pe}/\omega_{ci}+O(v_p), \tag{13}$$

by the electric field, Eq.(12), of the nonlinear magnetosonic wave. It should be noted that, since the potential jump is proportional to B^2, the $E\times B$ drift velocity of the trapped ions is proportional to B.

III. Simulation Model

We use a 2-1/2 dimensional fully relativistic, fully electromagnetic particle code. Spatial variation is allowed only in the x- and y-directions, with the z-direction being an ignorable coordinate, although the particles have three velocity components (v_x, v_y, v_z). The total grid size is $L_x\times L_y=512\Delta_g\times 32\Delta_g$, where Δ_g is the grid spacing. All lengths and velocities in the simulations will be normalized to Δ_g and $\omega_{pe}\Delta_g$, respectively, where ω_{pe} is the spatially averaged plasma frequency. The system is periodic in the y-direction and is bounded in the x-direction. The plasma simulation particles are confined in the region 30<x<482, being specularly reflected at x=30 and x=482.

When we solve Poisson's equation for the electrostatic fields we assume that there is no charge in the regions x<30 and x>482; i.e., the plasma is isolated with vacuum outside[13]. For the transverse electric and magnetic fields, we use an absorbing boundary condition[14]; outside the plasma region we have two absorbing regions, 0<x<30 and 482<x<512, where electromagnetic radiation leaving the plasma region is absorbed. By these procedures we avoid the interactions between the left and right sides of the plasma regions through the vacuum region.

The external magnetic field points in the z-direction with constant strength. The initial plasma density is constant in the y-direction (Fig.1(a)), and depends on x as

$$n_i=n_0 \qquad \text{for } 30<x<x_l,$$

$$n_i=n_0 exp(-(x-x_l)^2/2d^2) \qquad \text{for } x_l<x<x_r,$$

$$n_i=n_l \qquad \text{for } x_r<x<482.$$

In our simulations the constant n_0 is twice as large as the n_l, $n_0=2n_l$. Other parameters d, x_l and x_r are 17,67 and 84, respectively. The total number of the simulation particles is $N_i=N_e=65536$.

The momentum components $P_\sigma=m_j\gamma_j v_\sigma(\sigma=x,y,\text{or } z)$ are initially distributed according to an isotropic Maxwellian with average velocity zero, where γ_j is the relativistic gamma $=(1-v_j^2/c^2)^{-1/2}$. However, for the particles in the high density region, $30<x<x_l$, the x-component of the momentum P_x has the shifted Maxwellian distribution function with positive average velocity v_{ps}; these particles play a role of the piston which accelerates the particles in the main region, $x_l<x<482$, and excites the shock wave. An example of the ion phase-space plot (x,v_x) at t=0 is shown in Fig.1(b). In this case, the average velocity v_{ps} in the high density region is equal to the Alfven velocity v_a. The ions and electrons have the

same average velocity v_{ps} . We can change the shock strength by changing the magnitude of v_{ps} .

The simulation parameters are the following. The ion to electron mass ratio, m_i/m_e , is 50. The light velocity is c=4. The ion temperature is equal to the electron temperature, $T_i=T_e$, at t=0, with the electron thermal velocity $v_{Te}=(T_e/m_e)^{1/2}=0.5$ and the ion thermal velocity $v_{Ti}=0.07$. The strength of the external magnetic field is chosen so that $\omega_{ce}/\omega_{pe}=0.5$, where ω_{ce} is the electron cyclotron frequency. For these parameters, the beta value of the plasma which is the ratio of the plasma pressure to the magnetic energy is $\beta\sim 1/4$, and the Alfven velocity is $v_a=0.28$. The ion Larmor radius and the skin depth are $\rho_i=7.2$, and $c/\omega_{pe}=4$, respectively.

The electric and magnetic fields are normalized to $m_e\omega_{pe}^2\Delta_g/e$, and the electric potential is normalized to $m_e\omega_{pe}^2\Delta_g^2/e$, hence the normalized potential φ is expressed by the unnormalized potential φ_u as $\varphi=(e\varphi_u/T_e)(\lambda_{De}/\Delta_g)^2$. In the present case, $(\lambda_{De}/\Delta_g)^2$ is equal to 0.25, i.e., if, for instance, the normalized potential is equal to unity, the potential is 4 times as large as the electron temperature.

IV. Simulation Results

In this section we describe the time evolution of the shock and demonstrate the generation of the high-energy ions in IV.A. We study shock properties in detail in IV.B.

IV.A Ion Acceleration by Magnetosonic Shock Wave

We excite a large magnetosonic pulse by the instantaneous piston acceleration of the plasma; the ions and electrons in the high density

region, $30<x<x_l$, have average velocity $v_{ps}=v_a$ at $\omega_{pe}t=0$, and they push the plasma in the main region, $x_l<x<482$, in early phase. In Fig.2 we show the time evolution of the electron density profile $n_e(x)$ averaged over the y-direction at time $\omega_{pe}t$=219, 339, 459, *and* 579. By $\omega_{pe}t$=339, the propagating pulse is almost separated from the high-density plasma. The profiles of the pulse at $\omega_{pe}t$=339, 459, *and* 579 have the saw-tooth structure; the density has the steep gradient in the shock front with the width Δ being about 25, and behind the peak of the density, it decreases slowly. For this case ($v_{ps}=v_a$), the strong pulse propagates with the velocity $v=1.45v_a$, and with the density perturbation $\delta n/n\sim 0.5$. Once the shock is formed, the amplitude and the width are nearly constant.

Figure 3 shows the profiles of the magnetic field B(x) at $\omega_{pe}t$=320, *and* 560, and the electric potential $\varphi(x)$ at $\omega_{pe}t$=339, *and* 579. They are averaged over the y-direction, and time-averaged over a few electron plasma periods. The magnetic field has quite similar structure with the density profile; the perturbation of the magnetic field is $\delta B/B\sim 0.5$ and the width of the shock front is $\Delta\sim 25$. The potential has large positive value at the peak. It rises rapidly in the shock region by an amount $\delta\varphi\sim 2.4$, which is about 10 times as large as the ion temperature. It is interesting to note that there are two peaks in these profiles. The profiles oscillate and undergo a damped approach to the values far behind the shock. This implies that a soliton has changed into the quasi-shock as a result of some dissipation[7-9].

In Fig.4 we show the phase-space plots (x,v_x) and (x,v_y) at $\omega_{pe}t$=440 for the ions. Near the left boundary of the plasma region, $x\sim 30$, there are high-energy ions. Such high-energy ions exist there because we initially gave the average velocity v_{ps} to the particles near the left boundary. They are oscillating and the plasma there may be in turbulent state. In

the shock region, $x\sim250$ at $\omega_{pe}t=440$, there are ions which are resonantly interacting with the wave. They are trapped by the large potential in the shock region and are accelerated in the y-direction (parallel to the wave front) as well as in the x-direction. The trapped ions gain momentum in the negative y-direction(Fig.4(b)). The maximum velocity v_{yi} is $v_{yi}\sim-0.6\sim-2v_{a1}$. We can estimate the electric field E_x from Fig.3 as $E_x\sim0.1$, which gives the maximum attainable velocity by the $v_p\times B$ acceleration as $v_{yi}\sim cE_x/B+O(v_p)\sim-0.6$. Therefore, our simulation is in good agreement with the theoretical prediction for the maximum velocity[1]. It is noted that, since E_x is positive in the shock region, the $E_x\times B$ drift is in the negative y-direction, while in the fluid model, the ion velocity v_{yi} is positive and very small as Eq.(8) predicts. Hence, the generation of the ions with large negative v_{yi} in the simulation is due to the kinetic effect (the $v_p\times B$ acceleration).

We show in Fig.5 the ion phase-space plots (v_x, v_y) at time $\omega_{pe}t=$ 0, and 520. These are the plots of ions which are ,at $t=0$, in the main region $x_l<x$; from Fig.5 we have eliminated the ions which are initially in the region $30<x<x_l$ with average velocity $v_x=v_{ps}$ because we are interested in the acceleration of ions which are,in average, at rest before the shock arrives. We clearly see the high-energy ions in Fig.5(b). After the detrapping, the high-energy ions rotate on the (v_x, v_y) plane with the ion cyclotron frequency with the modulus of the velocity nearly constant. As the shock propagates, the electric field E_x continues to generate the high-energy ions as long as the amplitude is large.

In the case of the magnetosonic shock wave, the $v_p\times B$ acceleration heats the ions mainly as shown in Fig.6 where the kinetic energies of the ions and electrons are plotted as a function of the time. Here we measured the kinetic energy of the particles which are initially in the main

region, $x_1<x$. At $\omega_{pe}t=600$, the increase in the ion kinetic energy ΔK_i is about 8 times as large as the increase in the electron kinetic energy ΔK_e.

IV.B Propagation Properties of Shock Wave

We now study the dependence of shock properties on the shock strength. We show in Fig.7 the (x,t) diagram of the shock front for four different amplitudes. The slope of the line gives the propagation speed of the nonlinear pulse. The line a is the theoretical curve for an infinitely small pulse propagating with the Alfven speed v_{a1}. The propagation speed is rather constant in time. In the fastest case in Fig.7, the Alfven Mach number, M_a, is $M_a=1.57$. The shock shown in the previous figures, Figs.2-6, is the second fastest case with $M_a=1.45$.

In Fig.8 we plot the amplitude of the pulse as a function of the Mach number M_a. The white circles show the ratio of the maximum magnetic field strength to the magnetic field strength ahead of the shock, B_m/B_1, observed in the simulation, and the triangles denote the ratio of the maximum density to the density ahead of the shock, n_m/n_1. The line s is the theoretical curve for the magnetosonic soliton, $B_m/B_1=2M_a-1$, in a cold plasma, while the line RH is obtained from the Rankine-Hugoniot relation of the shock theory for the low beta plasma,

$$B_m/B_1=n_m/n_1=8/\{1+5/2M_a+[(1+5/2M_a)^2+8/M_a]^{1/2}\}. \qquad (14)$$

The observed magnetic field ratio takes almost the same value with the density ratio, and they are between the Rankine-Hugoniot curve and the soliton curve. If we take into account the effects of the plasma pressure, the theoretical curve s for the soliton may be closer to the simulation data. Since the beta value is about 1/4, the speed of the infinitely small

pulse may be $(1.2\text{-}1.3)M_a$.

The theoretical soliton width of the cold plasma is given by Eq.(11). According to the kinetic theory[11,12], the soliton width is multiplied by $(1+(m_i/16m_e)\beta_i)^{1/2}$ or by $(1-3\beta_e/4)^{1/2}$, depending on the amplitude. In our simulations, the mass ratio is $m_i/m_e=50$, and the beta value is $\beta_i=\beta_e=0.13$, hence these factors are near unity; the kinetic and fluid theories give almost the same value for the width. Hence we compare our simulation result with Eq.(11). As we have seen in Figs.2-3, the scale length of the shock front is much smaller than the one behind the peak of the pulse. We measure the width of the front of the pulse. In Fig.9 the shock width thus measured is plotted as a function of the shock strength, M_a-1. The shock width Δ scales as $(M_a-1)^{-1/2}$ as predicted by Eq.(11). The value is, however, about 6 times as large the one given by Eq.(11). One reason may be that the ion Larmor radius is larger than the skin depth, $\rho_i/(c/\omega_{pe})=1.8$, in our simulations.

We show in Fig.10 the potential difference, $\delta\varphi=\varphi_2-\varphi_1$, as a function of the magnetic field jump, B_2/B_1. The white circles are the simulation results, and the solid line is the theoretical curve for the soliton, Eq.(10'). The observed potential $\delta\varphi$ increases proportionally to the pulse strength B_2/B_1, and is in very good agreement with the theory. For the case of $B_2/B_1=1.75$, the potential difference $\delta\varphi$ is 3.35, i.e., the potential energy is about 13 times as large as the initial ion temperature.

As we have seen in Eq.(12), the electric field strength is strongly dependent on the shock strength. Therefore the number of the high-energy ions increases rapidly with the shock strength. Figure 11 shows the ion phase-space plots (x,v_y) and (v_x,v_y) for the weak pulse with $M_a=1.23$ (Figs.11(a) and (b)) and for the strong shock with $M_a=1.57$

(Figs.11(d)-(f)). For the weak shock case, we find no trapped ions in Fig.11(a), and hence there are no high-energy ions in the phase-space plot (v_x, v_y) in Fig.11(b). On the other hand, the strong shock reasonantly interacts with many ions (Fig.11(c)), and generates high-energy ions as shown in Figs.11(d)-(f). The high-energy ions with positive v_x near the left plasma boundary in Fig.11(c) exist because the particles in the region $30<x<x_l$ had the average velocity v_{ps} at $t=0$. Since we are not interested in those particles, the ions which are initially in the region $30<x<x_l$ are eliminated from Figs.11(b) and (d)-(f) as in Fig.5. The trapped ions are accelerated in the positive x- and negative y- direction. After they are detrapped, they rotate clockwise on the (v_x, v_y) plane. The high-energy ions form fan-shaped distribution on the (v_x, v_y) plane (Figs.11(d)-(e)). Since the high-energy ions are generated continuously, the fan-shaped area of the high-energy ions increases gradually, and eventually becomes a circle in a few ion cyclotron periods (Fig.11(f)). In this strong shock case, the radius of the circle of the high-energy ions on the (v_x, v_y) plane is about 0.75, which is about 10 times as large as the initial ion thermal velocity, $v_{ti}=0.07$, and 2.7 times as large as the Alfven velocity, $v_a=0.28$.

V. Summary

We have studied the $v_p \times B$ acceleration of the ions by the magnetosonic shock wave propagating in the direction perpendicular to the magnetic field by using the 2-1/2 dimensional fully relativistic, and fully electromagnetic particle code. Simulation results are compared with the theory in detail. It is found that the simple nonlinear wave theory

based on the cold plasma model well describes the propagation properties of the nonlinear pulse except for the effects of the resonant particles. In particular the potential difference in the nonlinear magnetosonic pulse is derived theretically in terms of the magnetic field and the plasma variables ahead of the shock. The potential difference can be quite large compared with the ion temperature. Since the potential jump is proportional to B^2, the $E\times B$ drift velocity of the trapped ions is proportional to B. The magnitude of the potential difference observed in the simulation is in good agreement with the theoretical prediction.

The pulse is excited by the instantaneous piston acceleration in the simulation. We impose no external currents or electric fields to sustain the pulse propagation, hence the evolution of the wave is totally self-consistent.

It is demonstrated that the self-consistent magnetosonic pulse with large amplitude can give rise to the $v_p\times B$ acceleration of the ions. The large amplitude pulse traps some ions and strongly accelerates them in the direction parallel to the wave front. The ions are detrapped when their velocities become of the order of the sum of the $E\times B$ drift velocity and the wave phase velocity. Because of the ion heating by this mechanism, the pulse develops into the magnetosonic shock wave in a collisionless plasma. The plasma variables such as the magnetic field and the plasma density have the saw-tooth structure.

In our case the shock is formed in a collisionless plasma by the dissipation due to the $v_p\times B$ acceleration not by the anomalous resistivity arising from micro-instabilities. The plasma was stable against the micro-instabilities in the shock region. One reason for the stability may be that perturbations with finite k_z ($k_zB\neq 0$) are inhibited in our 2-1/2 dimensional model. Hence the dangerous modes such as the lower hybrid

drift instability can not grow[15] .

References

1). R.Sugihara and Y.Midzuno, J. Phys. Soc. Japan 47, 1290 (1979), see also, R.Z.Sagdeev and V.P.Shapiro, Pis'ma Zh. Eksp. Teor. Fiz. 17,387 (1973) (JETP Lett. 17, 279 (1973)).

2). R.Sugihara, S.Takeuchi, K.Sakai, and M.Matsumoto, Phys. Rev. Lett. 52, 1500 (1984).

3). B.Lembege, S.T.Ratliff, J.M.Dawson, and Y.Ohsawa, Phys. Rev. Lett. 51, 264 (1983).

4). B.Lembege and J.M.Dawson, Phys. Rev. Lett. 53, 1053 (1984).

5). J.Adlam and J.Allen, Phil. Mag. 3, 448 (1958).

6). L.Davis, R.Lust, and A.Schluter, Z.Naturforsch. 13a, 916 (1958).

7). R.Z.Sagdeev in Reviews of Plasma Physics, vol.4, p.65, edited by M.A.Leontovich (Consultants Bureau, New York, 1966).

8). D.A.Tidman and N.A.Krall, in Shock Waves in Collisionless Plasmas, chap.3 (John Wiley & Sons, Inc. New York, 1970).

9). C.S.Morawetz, Phys. Fluids 4, 988 (1961).

10). Y.Ohsawa and J.M.Dawson, Phys. Fluids 27, 1491 (1984).

11). C.S.Gardner and G.K.Morikawa, Commun. Pure and Appl. Math. 18, 35 (1965).

12). N.A.Krall, Phys. Fluids 12, 1661 (1969).

13). V.K.Decyk and J.M.Dawson, J. Comp. Phys. 30, 407 (1979).

14). P.C.Liewer, A.T.Lin, J.M.Dawson, and M.Z.Caponi, Phys. Fluids 24, 1364 (1981).

15). P.C.Liewer and N.A.Krall, Phys. Fluids 16, 1953 (1973).

Figure Captions

Fig.1 Initial plasma density profile and ion phase-space plot (x, v_x). The particles in the high-density region have the average velocity v_{ps} at $t=0$.

Fig.2 Time evolution of electron density profile. The pulse propagating in the positive x-direction develops into the shock.

Fig.3 Profiles of the magnetic field at $\omega_{pe}t$ = 320 and 560, and the electric potential at $\omega_{pe}t$ = 339 and 579. Two peaks are seen in the quasi-shock form.

Fig.4 Ion phase-space plots (x, v_x) and (x, v_y). Resonant ions are accelerated in the shock region $x \sim 250$.

Fig.5 Ion phase-space plots (v_x, v_y) at $\omega_{pe}t$ = 0 and 520. The high-energy ions are being generated.

Fig.6 Time variation of ion and electron kinetic energies. The $v_p \times B$ acceleration heats the ions mainly.

Fig.7 (x, t) diagram for the nonlinear pulse. The line a is for the infinitely small pulse with propagation speed v_{a1}.

Fig.8 Pulse amplitude versus propagation speed. The line s is the theoretical curve for the soliton in a cold plasma, and the line RH is the Rankine-Hugoniot relation for the low beta plasma.

Fig.9 Pulse width versus pulse strength. Width varies with $(M_a-1)^{-1/2}$.

Fig.10 Potential difference versus magnetic field jump. The solid line is the theoretical curve for the soliton in a cold plasma.

Fig.11 Ion Phase space-plots for weak pulse ((a) and (b)), and for strong pulse ((c)-(f)). For the weak pulse with B_m/B_1=1.17, no resonant ions are found. For the strong pulse with B_m/B_1=1.75, many high-energy ions are generated.

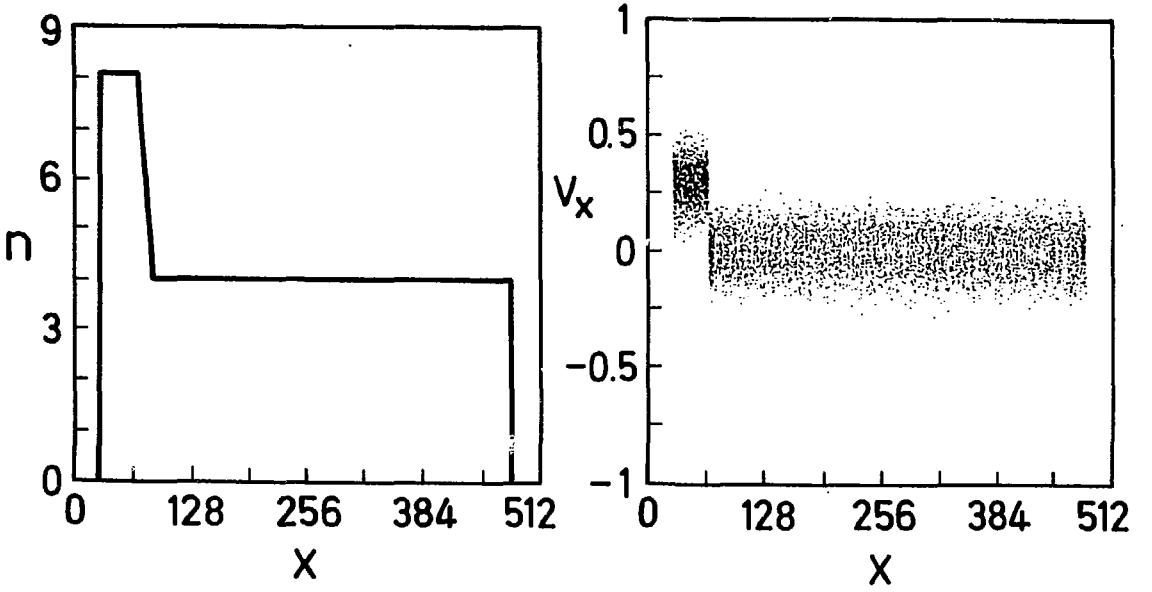

Fig.1

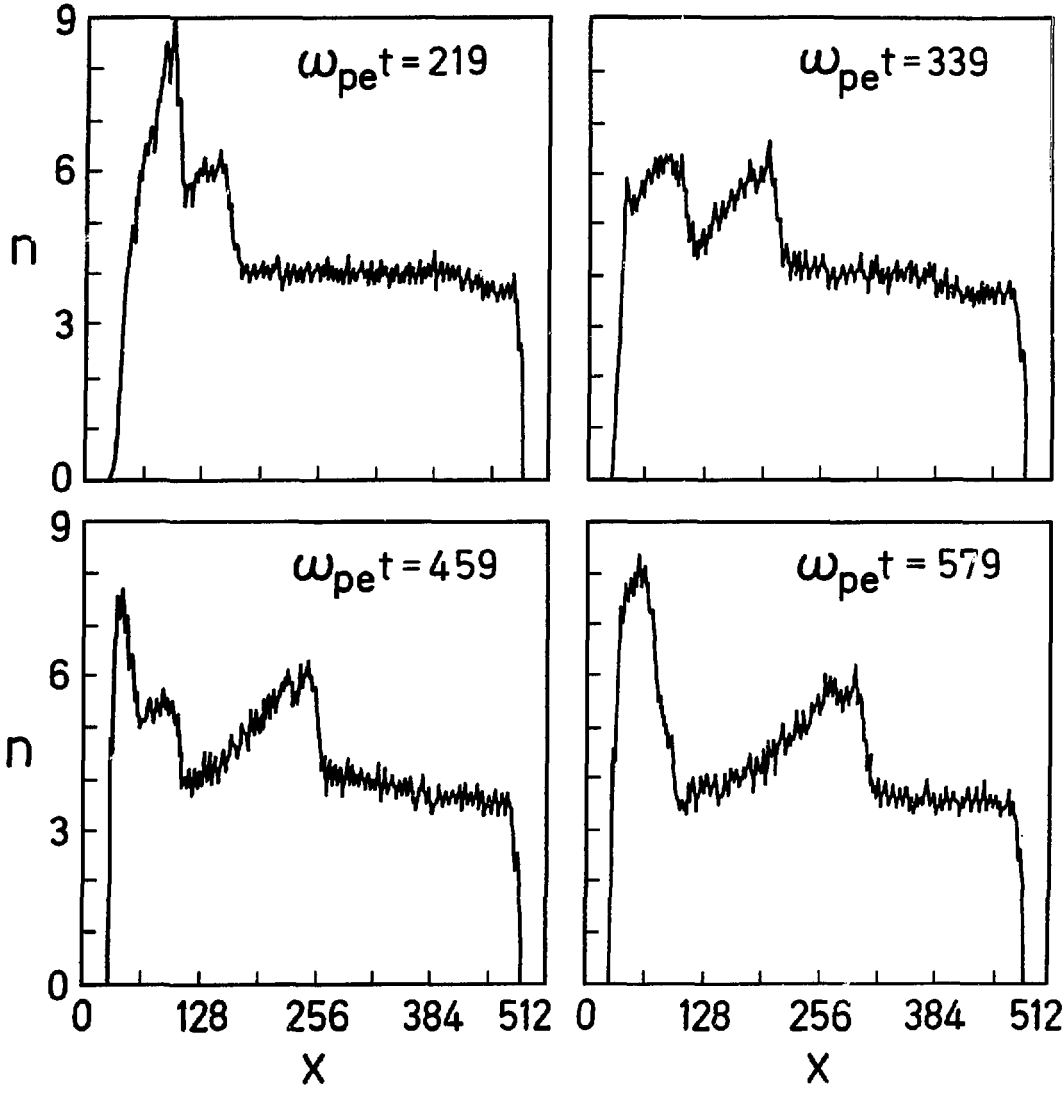
$\omega_{pe}t = 219$
$\omega_{pe}t = 339$
$\omega_{pe}t = 459$
$\omega_{pe}t = 579$
n
n
9
6
3
0
0
128
256
384
512
X
X

Fig.2

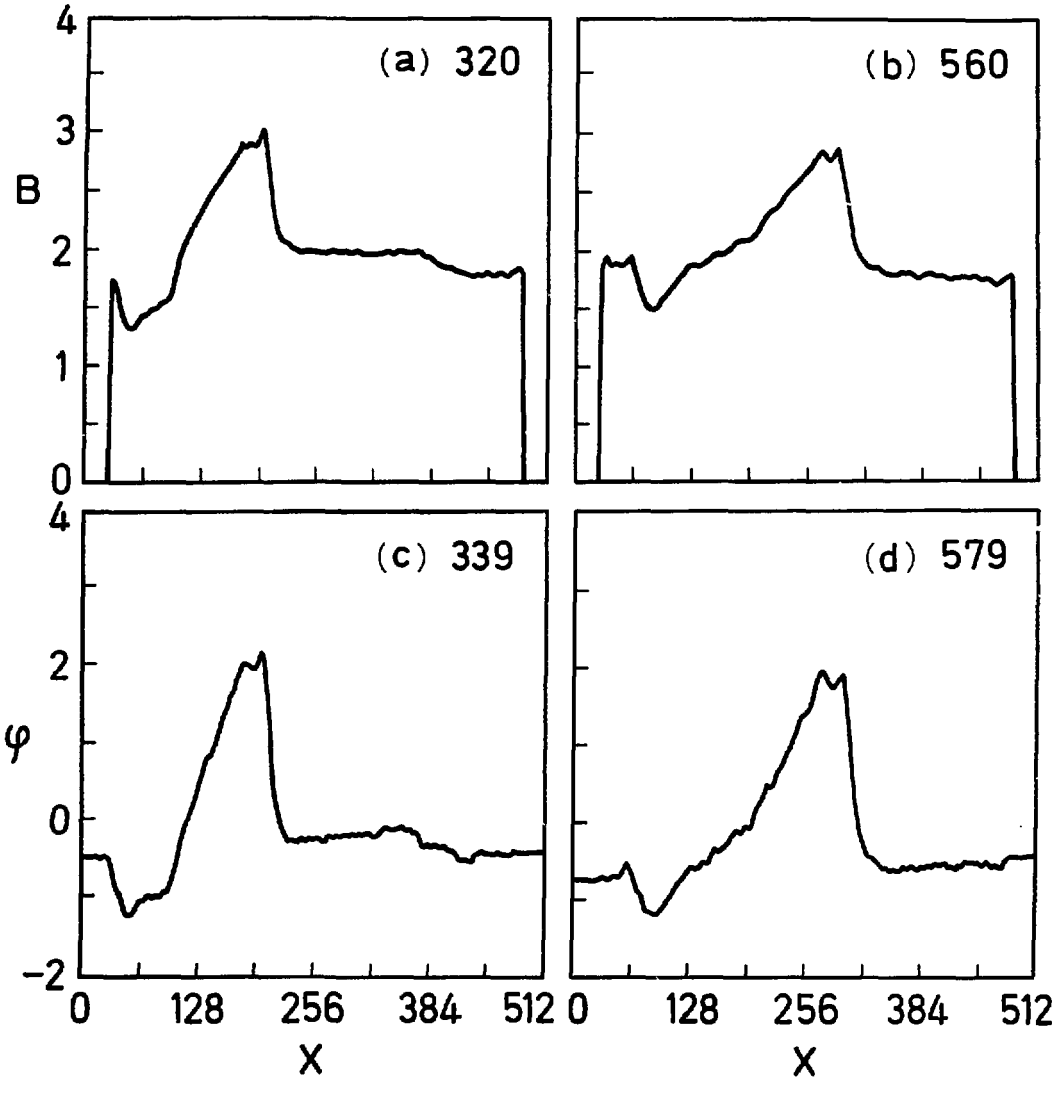

Fig.3

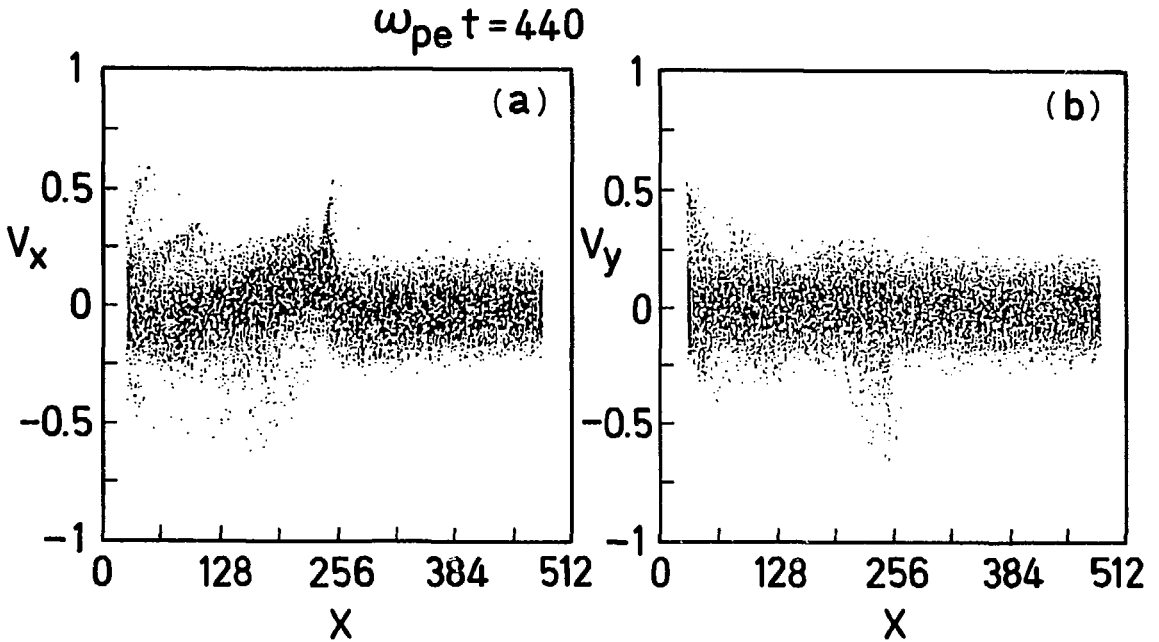

Fig.4

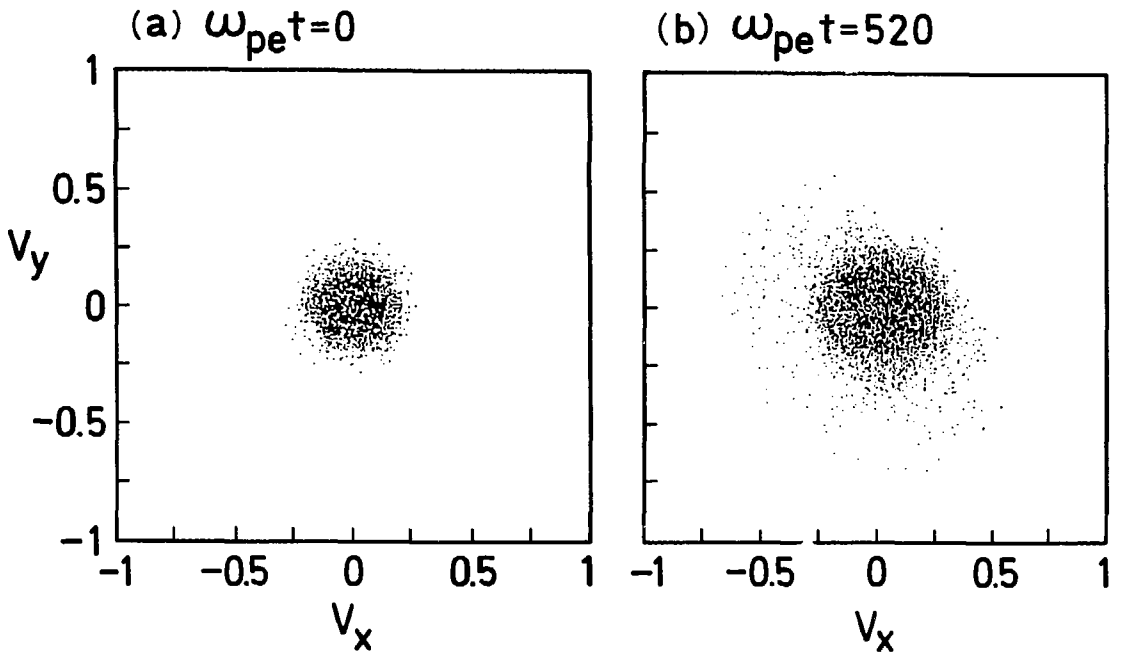

Fig.5

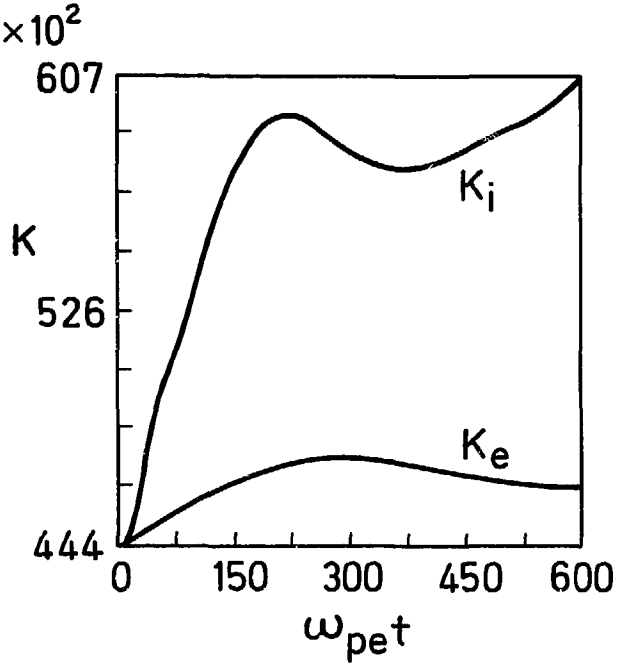

Fig.6

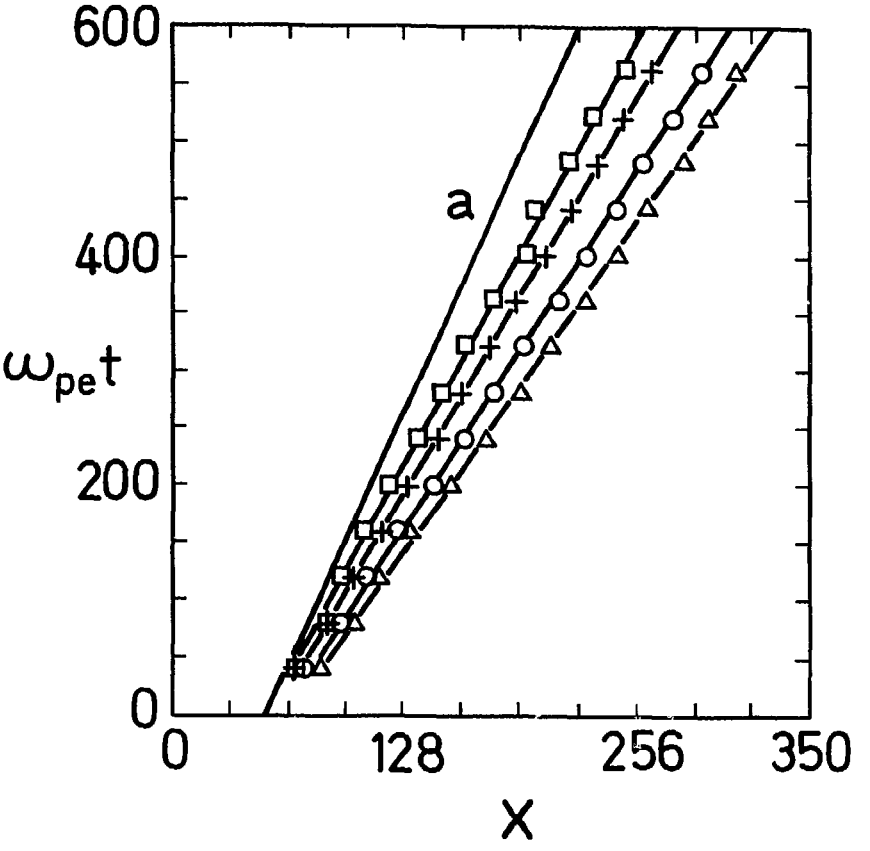

Fig.7

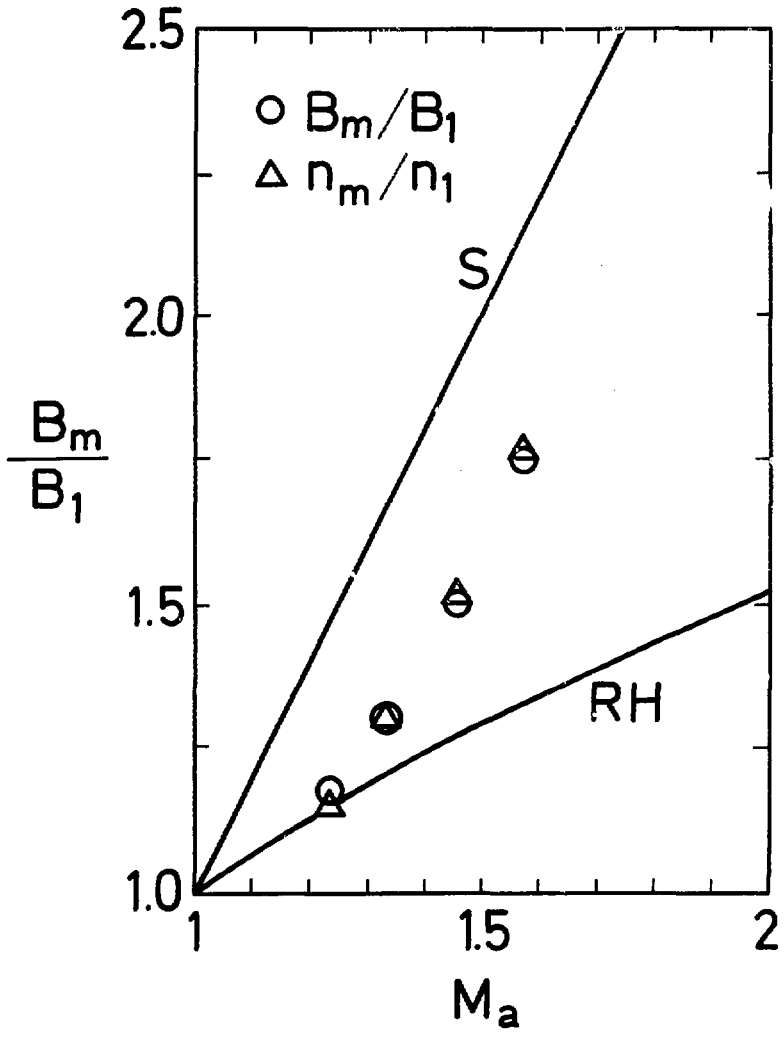

Fig.8

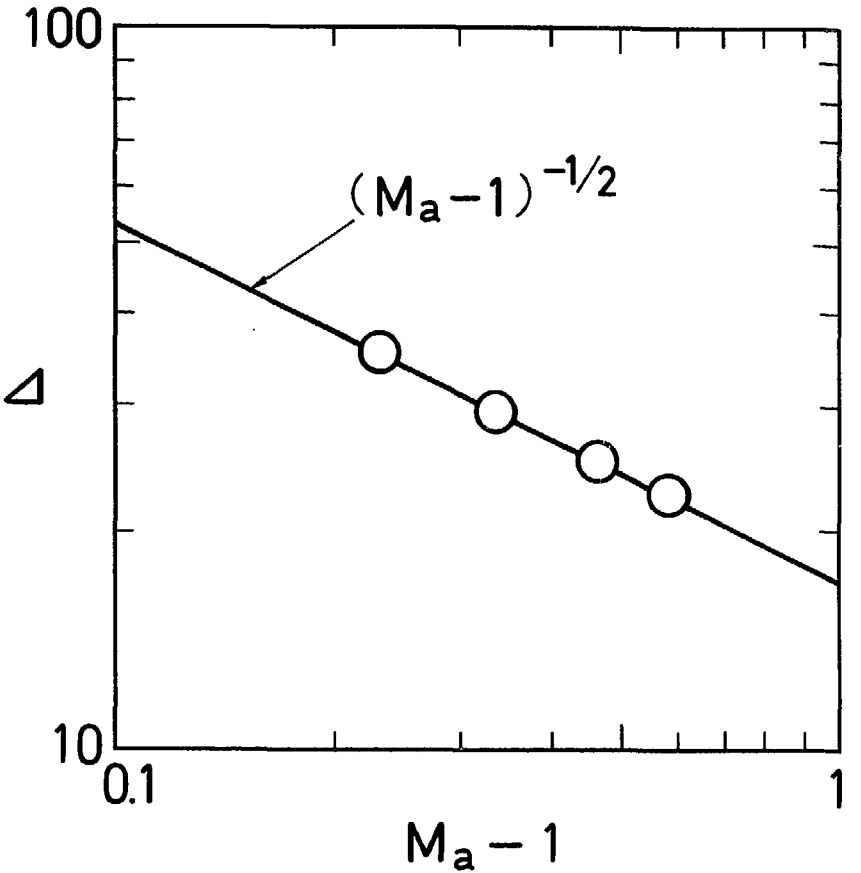

Fig.9

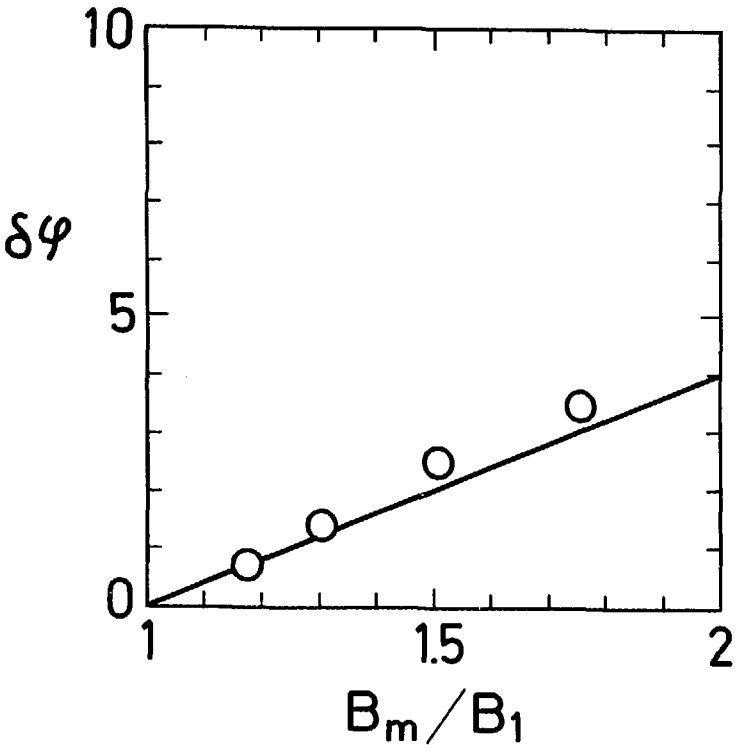

Fig.10

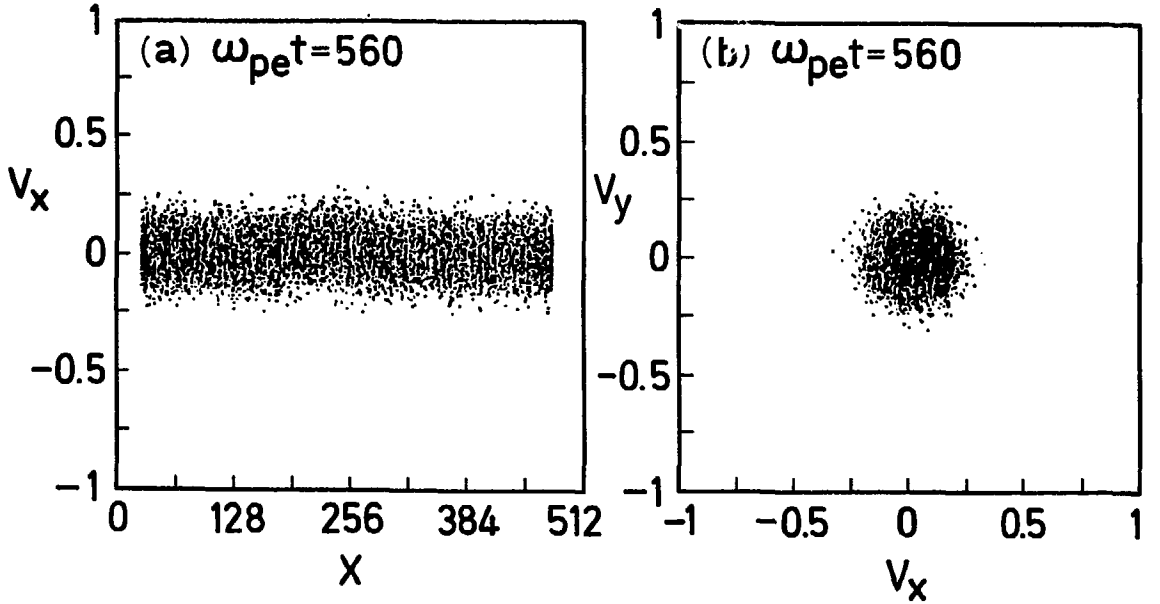
(a) $\omega_{pe}t=560$
(b) $\omega_{pe}t=560$
V_x
V_y
1
0.5
0
−0.5
−1
0
128
256
384
512
X
−1
−0.5
0
0.5
1
V_x

Fig.11(a)-(b)

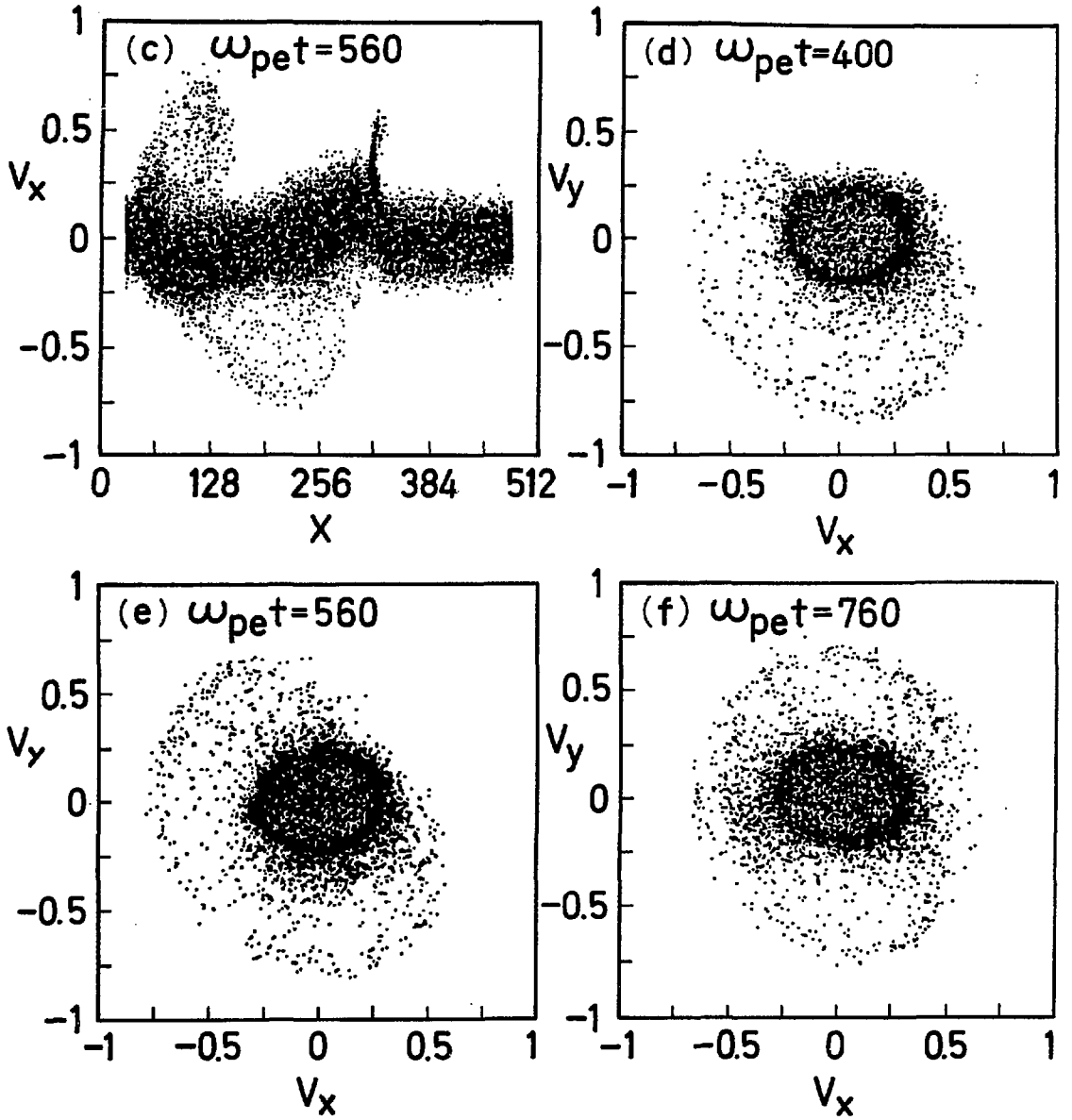
(c) $\omega_{pe}t=560$
(d) $\omega_{pe}t=400$
(e) $\omega_{pe}t=560$
(f) $\omega_{pe}t=760$
V_x
V_y
X
1
0.5
0
-0.5
-1
0
128
256
384
512

Fig.11(c)-(f)